# Core crush criterion to determine the strength of sandwich composite structures subjected to compression after impact

Bruno Castanié [a,*], Yulfian Aminanda [b], Christophe Bouvet [a], Jean-Jacques Barrau [a]

[a] Université de Toulouse, UPS/LGMT (Laboratoire de génie mécanique de Toulouse), Bat 3PN, 31062 Toulouse Cedex, France
[b] Mechanical Engineering Department of IIUM, Jl. Gombak P.O. Box 10, 50728 Kuala Lumpur, Malaysia

*Keywords:*
Impact
Sandwich structures
Compression after impact
Honeycomb core crush
Finite element analysis

ABSTRACT

In this study a core crush criterion is proposed to determine the residual strength of impacted sandwich structures. The core of the sandwich is made of a Nomex Honeycomb core and the faces are laminated and remain thin. The mechanism of failure of this kind of structure under post-impact compressive loading is due to interaction between three mechanical behaviors: geometrical nonlinearity due to the skin's neutral line off-set in the dent area, nonlinear response of the core and damages to the skins. For the type of sandwich analysed in this study, initially the core crushes at the apex of the damage. Using a finite element discrete modelling of the core previously proposed by the authors, the load corresponding to the crushing of the first cell can be computed and it gives the value of the residual strength for our criterion. Some geometric and material hypotheses are assumed in the damaged area mainly based on non-destructive inspection (NDI). The criterion is then applied to tests modelled by Lacy and Hwang [Lacy TE, Hwang Y. Numerical modelling of impact-damaged sandwich composites subjected to compression after impact loading. Compos Struct 2003;61:115–128]. It is shown that the criterion allows a good prediction of the tests except in the case of very small dents. Several sensitivity studies on the assumptions were made and it is shown that using this approach, the criterion is robust.

## 1. Introduction

Sandwich structures exhibit static properties like high stiffness-to-weight ratio and high buckling loads that are of great importance in the aeronautics field. Although their properties have been known since the thirties, the current applications remain limited to secondary structures such as surface controls or floor panels or to a small number of primary aircraft structures such as the Beechcraft Starship (Hooper [2]). In fact, the limitations are linked to the cost and reliability of manufacturing (Sheahen et al. [3]), moisture problems and to the general lack of knowledge of the effects induced by impact damages (drop in strength up to 50% (Abrate [4]). To meet the requirements for certification, aircraft manufacturers mainly validate their components experimentally by using compression after impact tests (CAI) on representative specimens (Tomblin et al. [5], Castanié et al. [6]). This empirical method is costly and therefore reliable and not too conservative computation methods are needed. Moreover, impacts often occur in service or during maintenance operations and aircraft manufacturers should give rapid responses to the operating company. Thus, the objective of the present method is to provide a relatively simple and efficient finite element model integrating the core crush criterion.

The type of damages occurring during low velocity-low energy impacts are well known [7,8]: core crush, skin fractures or delaminations and a residual dent depending upon the energy level. During compression after impact using hemispheric impactors, generally speaking, the form of the print becomes elliptical and simultaneously the dent depth increases [6,9–11]. Then a crack appears at the summit of the ellipse causing the failure of the specimen except in the case of a redundant structural test rig. So the analysis of the tests shows that the phenomenon occurring during CAI is due to interaction between three mechanical behaviors:

- A geometrical nonlinearity due to the skin's neutral line off-set in the dent area.
- A nonlinear response of the core due to the crushed state and the classical "with peak" response of the undamaged area.
- The response of the skin due to its type of damage after impact: delamination or crack growth.

Theses nonlinearities are at the origin of the difficulties encountered to model the phenomenon. Some analyses were analytical and based on wrinkling type models like those of Minguet [12] or more recently Xie and Vizzini [13,14]. In 1997, Guedra-

* Corresponding author. Tel.: +33 (0)5 62 17 81 16; fax: +33 (0)5 61 55 8178.
*E-mail address:* bruno.castanie@isae.fr (B. Castanié).

Degeorges [15] presented a nonlinear finite element model able to represent the evolution of the damage in the core during CAI by remeshing it. He pointed out the fact that the damage progression is linked to a compression over-stress that appears in the core and on the crush propagation line. Other finite elements models were proposed by Zenkert et al. [16] or by Lacy and Hwang [1,17]. In any case, the core is modelled by a continuum and the authors focused on the skin failures or wrinkling [18] to determine the compressive strength of the impacted sandwich.

Recently, after a phenomenological study [19,20], the authors have pointed out that during the compression of a low-density honeycomb core, due to a postbuckling mode of the cell walls, only the vertical edges of the hexagon cell take the compressive load. Thus, it is possible to model the core only by its vertical edges which leads to the creation of a grid of nonlinear springs in a finite element model. The compression law is based on a test on a sample of Nomex and can be enhanced by taking into account the effect of the interaction between the score and the skin [19,21]. This approach leads to a correct modelling of static indentation and dynamic impacts on sandwich structures with metallic skins [19,21]. Moreover, the approach was extended to the problem of compression after impact for the same kind of sandwich which enables the evolution of the residual dent and the ultimate strength to be predicted [19,22]. The core crush criterion was also proposed. The main results in this case will be detailed initially and then a nonlinear finite element using this approach will be proposed. Some materials and geometric assumptions will be assumed in relation to the tests and modelling of Lacy and Hwang [1] and NDI capabilities. Then a comparison with the tests results given by theses two authors [1] will be performed and finally, a sensitive study on the new proposed assumptions will be provided along with the conclusions and future perspectives.

## 2. Core crush criterion

In this section, the key points of previous publication [19,22] are summarized. Compression after impact tests and modelling were carried out on specimens with brass skins and Nomex honeycomb reinforced at both ends (Fig. 1). These specimens were previously indented on a flat support. The finite element model made with Samcef software (by Samtech Group [24]) can be seen Fig. 2. The core was modelled by vertical springs located at the vertical edges of the cells. Its behavior was obtained experimentally from cycled compression uniform loading test on a small block of Nomex honeycomb (see Fig. 3) and implemented using special features of the software. The skins were modelled by Mindlin elements and the mesh is refined in the impact area. It was necessary to model both skins to obtain the true balance of forces between the skins during the compression loading. The boundary conditions represented some knifes of the test rig on the impacted skin. The unimpacted skin was fully clamped. This was necessary because the discrete modelling of the core cannot take into account the shear stresses in the core and any flexural behavior of the sandwich. Thus, the non linear response of the unimpacted skin reported by Lacy and Hwang [1] cannot be captured. However, this hypothesis was weak and this non linear response is due to the asymmetric aspect of the sandwich caused by the impact and it seems not to have any influence on the residual strength. To model the tests correctly, it was necessary firstly to compute the indentation loading and unloading (thus obtaining the residual dent, the plastic residual stresses in the skin and the core crush area and depth) followed by the compression after impact loading simulated by imposing the displacements on the edges of the two skins of the sandwich (Fig. 2). By doing so, the evolution of the dent and the residual strength were predicted with a high degree of accuracy [19,22]. It was noticeable that the compression after impact behavior of sandwiches with metallic skins was almost the same as sandwiches with composite skins.

The core crush criterion was found by analysing the reaction of the first uncrushed springs placed in the dent evolution direction about the major axis of the ellipse and in the circumference of the residual print (see Fig. 4). The reaction of these springs (1–3) is initially very weak and does not increase much during the appearance and the progressive extension of the ellipse. After a drop of the spring force which is probably due to the appearance of a little bump that stretches the springs, a sudden increase of the compression force is observed until it reaches the critical force (the peak) for the first spring at the periphery (no. 1). It is very interesting to note that the collapse of this first edge occurs only shortly before the abrupt progression of the ellipse, which takes place when the second edge (spring no. 2) situated on the major axis of the ellipse, collapses in turn. Numerically, it is shown here that the advance of the defect coincides with the physical phenomenon of local core crush. Therefore, the collapse of the first edge situated on the major axis of the ellipse modelled by its spring can be proposed as the criterion for determining the computed residual strength. This criterion should logically always underestimate the experimental residual strength but not too much since the ellipse generally appears just before the catastrophic failure of the specimens. In the next paragraph, the approach will be developed to the case of composite skins.

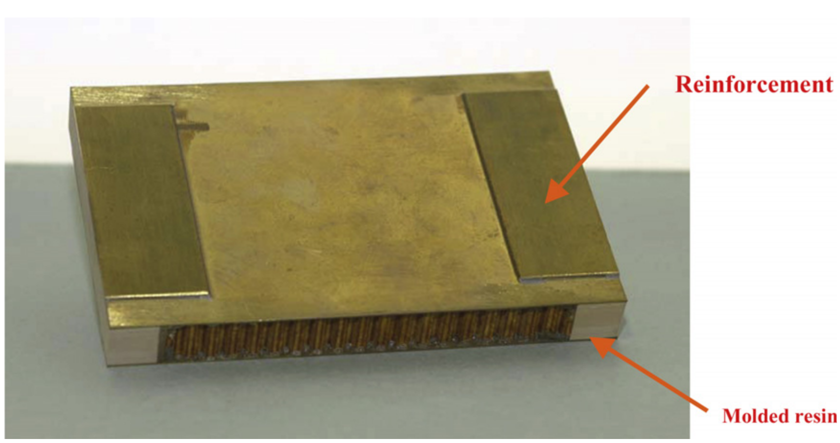


**Fig. 1.** Sandwich with metallic skins used for CAI Tests [19].

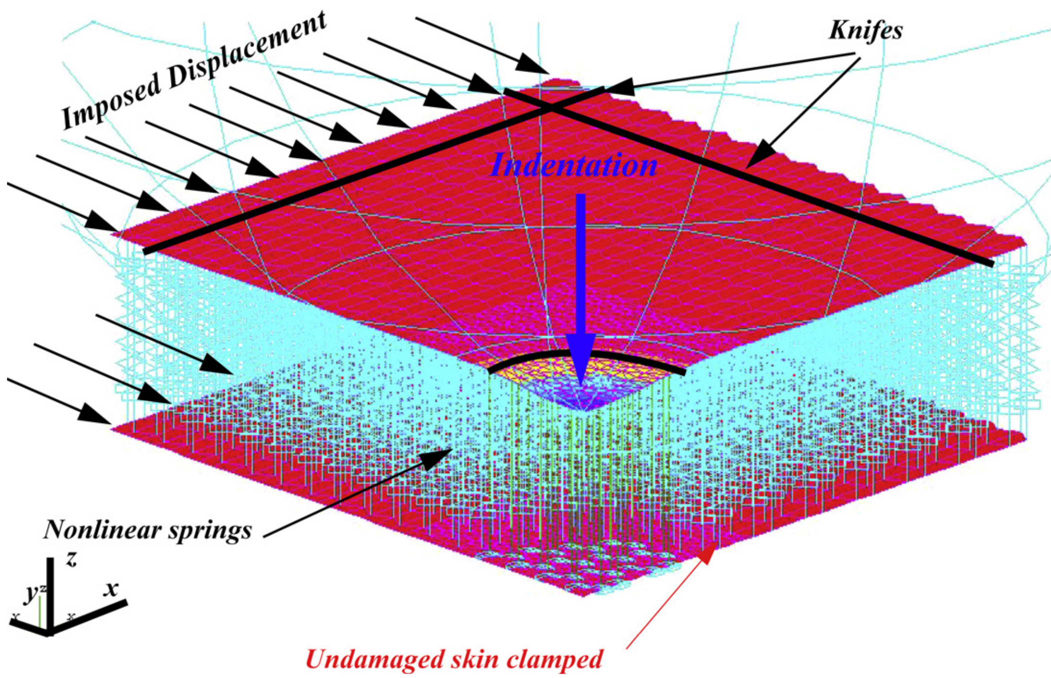


**Fig. 2.** Finite element model for compression after impact of sandwich with metallic skins.

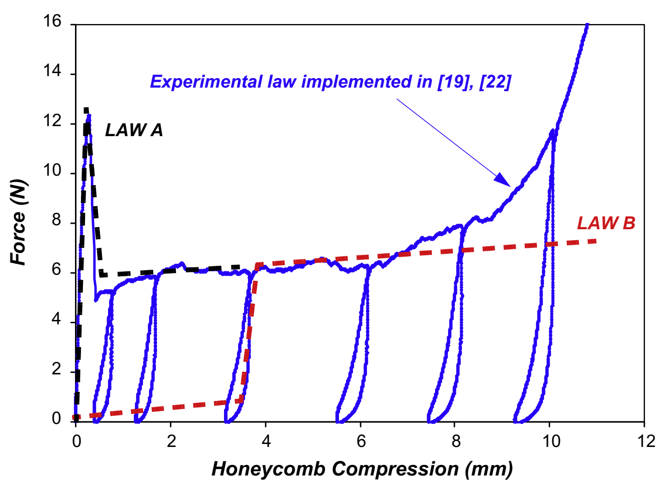


**Fig. 3.** Compression behavior of Nomex honeycomb with cycling.

## 3. Hypothesis and finite element model description

The finite element model reproduces globally the geometry of the specimens tested by Tomblin et al. [23] and modelled by Lacy and Hwang [1]. Only a quarter of the plate was modelled due to symmetries an the overall shape of what the model looks like Fig. 2. Thus the model size is $101.6 \times 127\ \text{mm}^2$. The geometry of the impact-damaged area is described Fig. 5 and the same notations as in [1,17] were used. For all the specimens reported here, the thickness of the core $t_C$ is 19.1 mm. The facesheet indentation depth $\delta_I$ and radius $R_I$ can be measured directly on specimens or on a real structure. In the new finite element model, the geometry of the dent is represented by coons surfaces [24].

The crushed core radius should be found by NDI techniques. It seems to be more difficult, in the case of sandwich structures, to determine the delaminated area. Thus, the degraded facesheet radius $R_F$ will be supposed equal to:

$$R_F = \frac{R_I + R_C}{2} \tag{1}$$

The core used in [23] is made of Nomex honeycomb, 48 kg/m$^3$, cell size 4.76 mm, transverse modulus $E$ equal to 137.9 MPa. Its maximum compressive strength is 2.41 MPa and the plateau stress is 1.03 MPa. Knowing all this values, for a given surface, it is easy to transform the continuum values into discrete ones for the springs located at the corners of the cells. The law "A" for an intact honeycomb under compression is given Fig. 6. The peak force is found to be equal to 23 N and the crush force equal to 9.86 N. The compression displacements are calculated directly from the strains given in [1]. This law is applied to the springs representing an intact core, i.e. located at a radius $R > R_C$. For the springs representing the crushed core, a law "B" is applied. These laws are of same type as in [1] and are in accordance with previous cycling test made by the authors on Nomex honeycomb (see Fig. 3 and [19,22]). The true value of the crushed core depth $\delta_C$ can, until now, be obtained by destructive sectioning. In an initial approach, the values given in [1] will be taken and applied to all the springs located in the crushed area (see Fig. 5). By doing so, the evolution of the crushed depth is not represented but an a posteriori sensitivity analysis will demonstrate that the influence of this parameter is weak. The residual force $F_{Residual}$ is also a weak parameter and was fixed to 1 N mainly for numerical stability reasons.

The skin is modelled by orthotropic Mindlin element (see Fig. 2). The skins of the specimens tested by Tomblin et al. [23] was a laminate made of Newport NB321/3K70P Plain wave carbon fabric. The stacking sequence was $[90/45]_n$ with $n = 1,2,3$ thus the skin thickness was equal to 0.4, 0.8 or 1.2 mm. According to the material characteristic of the ply given in [23], the orthotropic equivalent moduli were calculated and implemented in the finite element model for the element located at a radius $R > R_F$:$E_1 = E_2 = 47{,}200$ MPa, $E_{12} = 17{,}800$ MPa, $G_{12} = 17{,}800$ MPa, $\nu_{12} = 0.328$. The same transverse characteristics as in [1] were implemented.

For the damaged area, specific hypotheses are assumed concerning the stiffness matrix terms. For a given stacking sequence and for Mindlin's theory, this matrix can be written as

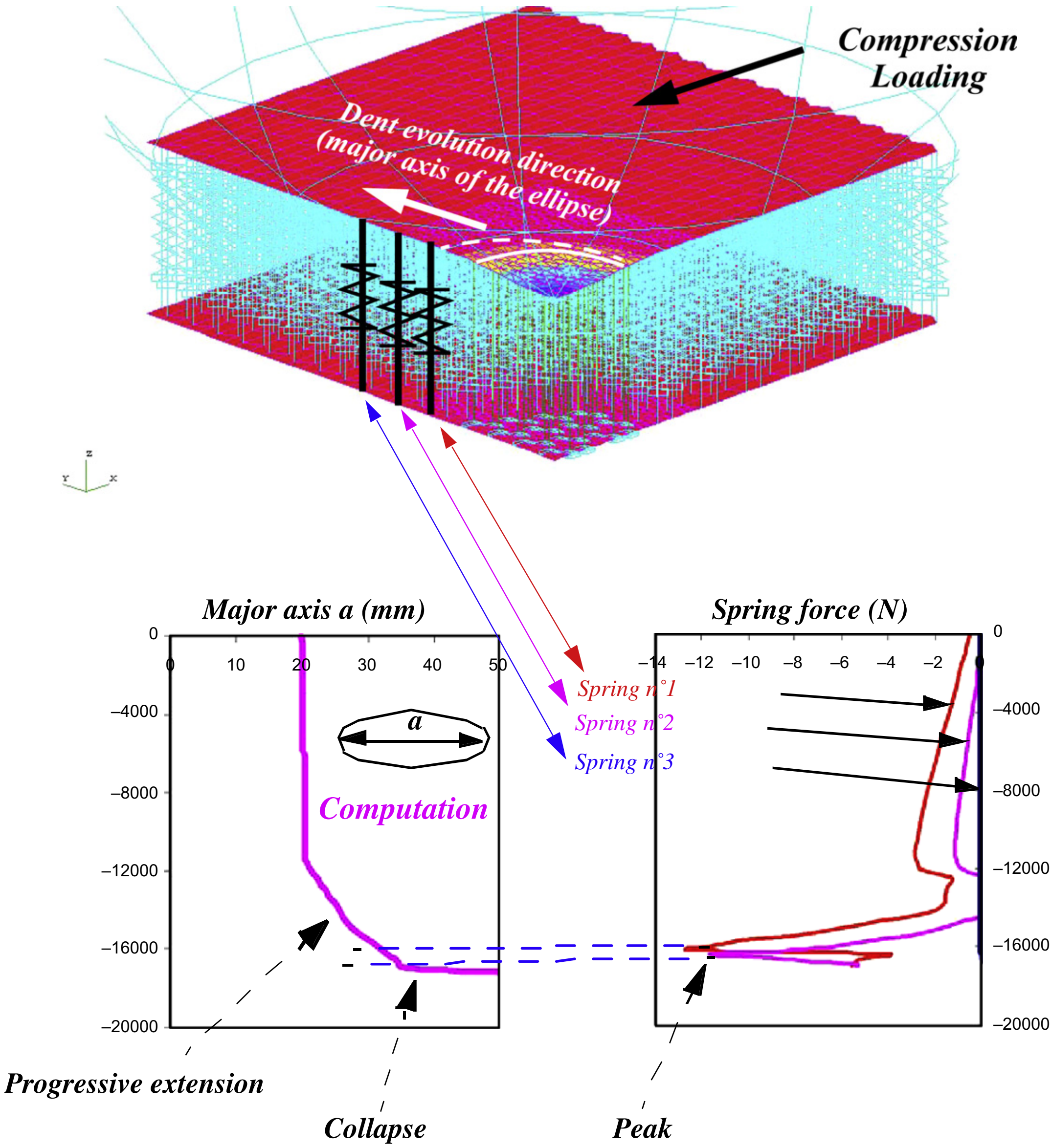


**Fig. 4.** Core crush criterion.

$$\begin{bmatrix} A & B & 0 \\ B & D & 0 \\ 0 & 0 & K \end{bmatrix} \quad (2)$$

[A] represents the membrane stiffness matrix. In the damaged area, this matrix should be affected by fibre breakages. Generally, these breakages are very localized at the centre of the impact, thus the matrix [A] is not modified.

[D] represents the bending stiffness matrix. For thin skins, it is possible to suppose the presence of a delamination located at the middle of the thickness and for $R < R_F$. This hypothesis leads to a decrease in bending stiffness equal to $1/(n+1)^2$ where $n$ is the number of delamination in the thickness. So, the bending stiffness matrix is here divided by four: [D]/4.

[B] represents the membrane-bending coupling stiffness matrix. When stacking sequences are symmetric, with respect to the middle surface, its value is zero. It is not the case for the stacking of the specimen, thus the same hypothesis is made and the coupling stiffness matrix is also diminished: [B]/4.

[K] represent the transverse shear stiffness matrix. It should be affected by matrix cracking but the influence on the residual strength is weak and [K] is not modified.

During the loading, the skin remains linear elastic and no damage growth is modelled. A geometric nonlinear analysis was made using a line-search method [24]. Different meshes were tested (quadrilateral cell or triangles) with different refinements showing a weak influence on the criterion. In the next paragraph, the model will be compared with 8 tests made by Tomblin et al. [23] for which all the data are available in [1].

## 4. Comparisons with tests

The data available in [1] are recalled in Table 1. Typical responses of the first uncrushed springs located in the major axis of the ellipse are given Fig. 7 and are extracted from the computation of case no. 4. Springs representing the intact cells reach the peak forces one after another, showing the mechanism of extension of the dent. However, only the load corresponding to the first peak has a physical meaning since it is assumed that there is no

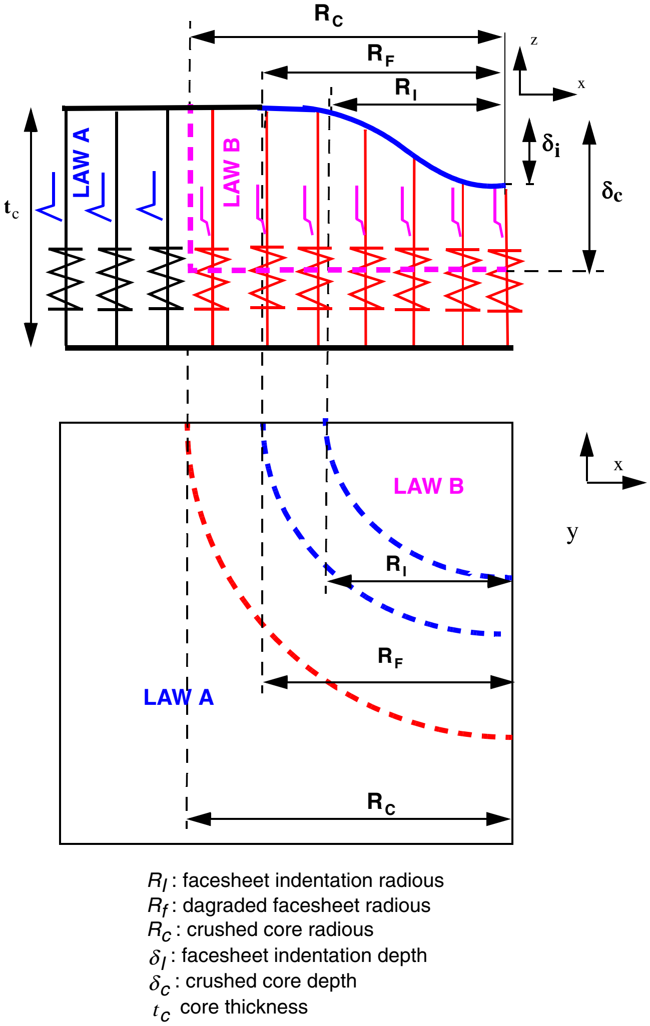


**Fig. 5.** Geometry of the impact-damaged region.

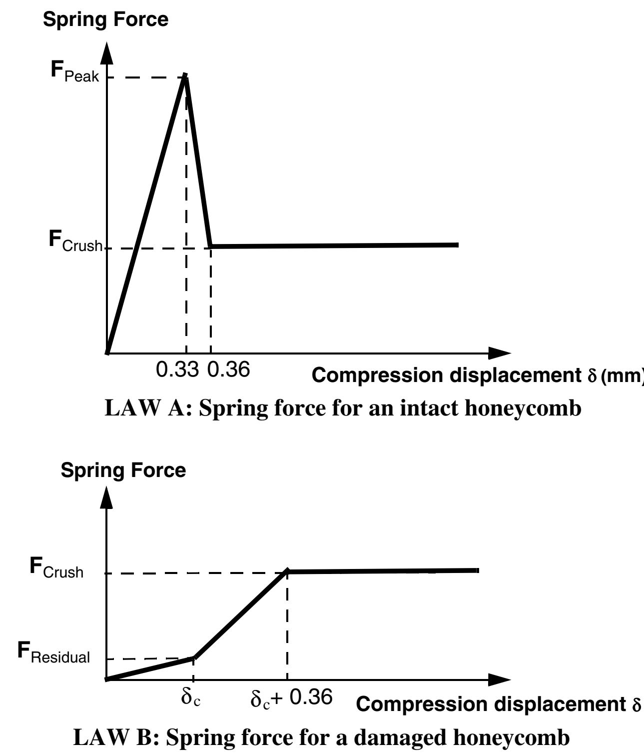


**Fig. 6.** Springs forces.

damage growth in the skin or appearance of a crack before the dent progression. The load displacement curve (not given) is globally linear and shows nothing in particular. When the first spring "crushes", the computed loading corresponding to the criterion is 291.5 N/mm. The second spring is crushed at 328 N/mm. The experimental failure of this sandwich was 317.5 N/mm. Thus the criterion underpredicts the failure by about 8%. The out-of plane displacement field for the criterion load can be seen Fig. 8 showing an extension of the dent in an ellipse shape. It is interesting to see the maximum strain field for this load in Fig. 9. Although, all of the skin is in compression, at the apex of the dent, one face of the skin is under tension (see Fig. 9) due to the local bending. The main strain reaches the very high level of 12,200 μ strains. Thus, this strain field implies that a crack could occur at this location which is in agreement with the failure scenario identified by several authors [5,6,11]. The same order of magnitude is frequently reached for thin skins of 0.4 and 0.8 mm but it becomes less important for thicker skins of 1.2 mm (about 8500 μ strains). A complementary analysis should be made on this point but the critical value of the opening crack for this materials remains to be found for this problem and cannot be provided by the authors.

In Table 2, the comparison is given for the 8 cases proposed by Lacy and Hwang [1]. Globally, the comparison is good and the residual strength is underpredicted by 8–25%. In two cases (3 and 7), the criterion did not work and overpredicts the experiment by 16 and 25%. The approach seems not to work in the case of low energy impact with small indenters that cause too small dents. The same behavior was pointed out in the case of metallic skins [19,22]. Maybe, for small dents, the geometrical imperfections are of same order of magnitude and should be taken into account. In case no. 5, the residual strength is underpredicted by 25%. The second springs collapses at a load of 315 N/mm (−11%) showing a very progressive extension of the dent. Moreover, for the criterion load, at the apex of the ellipse, the maximum tensile strain is only 8870 μ strains which suggests that no cracks appears at this load which could explain the underpredicted value by 25%. In such cases, the analysis should be coupled with modelling of skin damage and failure estimation as proposed in [17] to improve the estimation. However, the present model has the advantage of giving results within 10 min on a personal computer thanks to the use of springs and the linear behavior in the skins. This approach is thus suitable in an industrial context. To validate the approach, a sensitivity study is presented in the next paragraph.

## 5. Sensitivity analysis

The first influence to be studied is the hypothesis on membrane stiffness matrix. It was supposed that fibre breakage has a slight

**Table 1**
Impact characteristics and damage dimensions (reproduced from [1])

| Test | Skin thickness (mm) | Impactor Size (mm) | Energy (J) | $R_{\text{Indented}}$ (mm) | $R_{\text{Crushed}}$ (mm) | Indentation depth $\delta_C$ (mm) | Crushed depth $\delta_C$ (mm) |
|---|---|---|---|---|---|---|---|
| 1 | 0.4 | 25.4 | 6.7 | 10.2 | 15.2 | 2.3 | 5.9 |
| 2 | 0.4 | 76.2 | 7.2 | 15.9 | 25.4 | 0.4 | 6.2 |
| 3 | 0.8 | 25.4 | 6.7 | 3.2 | 15.9 | 0.8 | 3.8 |
| 4 | 0.8 | 25.4 | 20.3 | 12.7 | 21.7 | 3.2 | 7.8 |
| 5 | 0.8 | 76.2 | 7.2 | 9.5 | 28.6 | 0.4 | 4.5 |
| 6 | 0.8 | 76.2 | 28.2 | 34.4 | 48.7 | 4.2 | 6.6 |
| 7 | 1.2 | 25.4 | 6.7 | 9.5 | 19.1 | 0.6 | 4.1 |
| 8 | 1.2 | 76.2 | 11.1 | 12.7 | 28.6 | 0.6 | 4.8 |

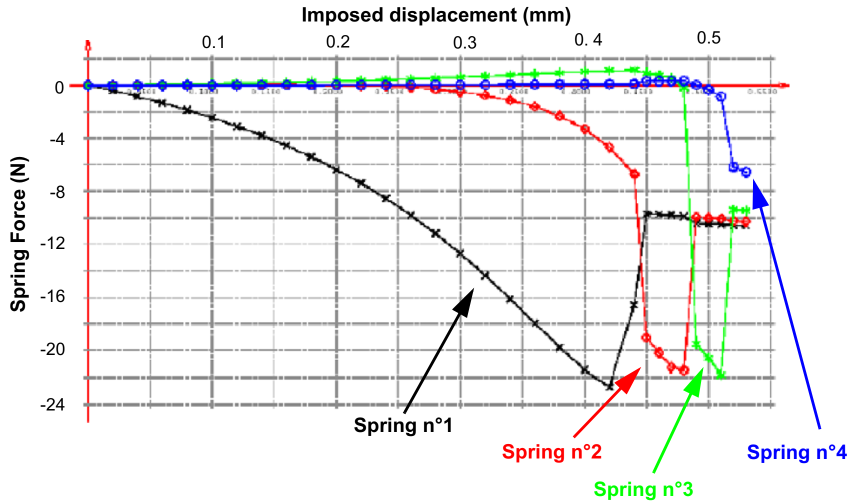


**Fig. 7.** Typical response given by the model (case no. 4).

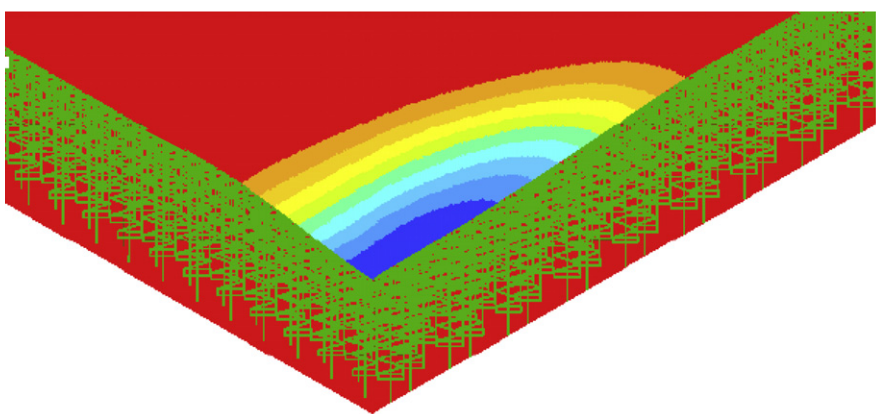

**Fig. 8.** Shape of the dent at the critical load.

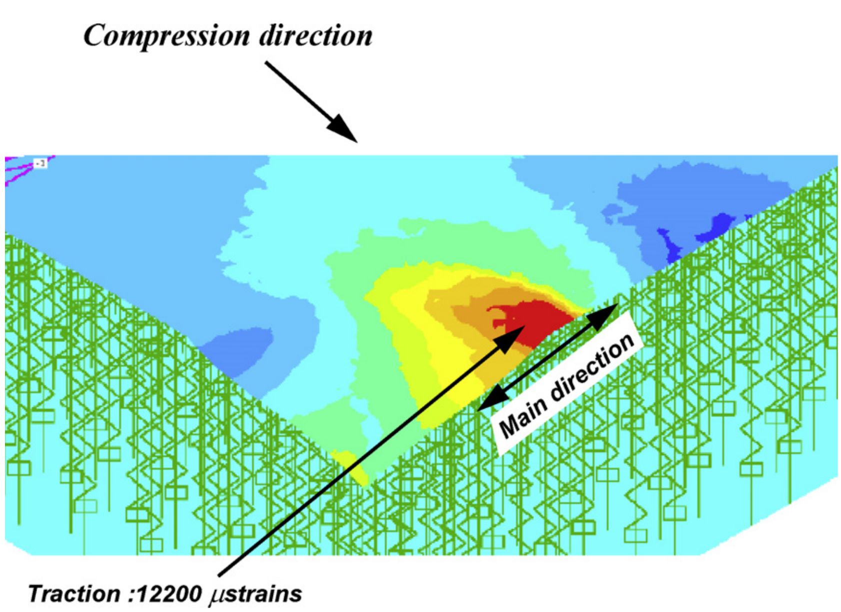


**Fig. 9.** Main strain field, lower skin, critical load 291.5 N/mm.

**Table 2**
Strengths predicted by the core crush criterion

| Test | Impactor size (mm) | Energy (J) | CAI test (N/mm) | CAI criterion (N/mm) | Difference (%) |
|---|---|---|---|---|---|
| 1 | 25.4 | 6.7 | 185.6 | 162 | −12 |
| 2 | 76.2 | 7.2 | 165.5 | 150 | −9.6 |
| 3 | 25.4 | 6.7 | 356 | 413 | +16 |
| 4 | 25.4 | 20.3 | 317.5 | 291.6 | −8.15 |
| 5 | 76.2 | 7.2 | 354.5 | 265 | −25 |
| 6 | 76.2 | 28.2 | 236.9 | 196 | − 17.3 |
| 7 | 25.4 | 6.7 | 482.6 | 600 | +25 |
| 8 | 76.2 | 11.1 | 429.6 | 398 | −7.3 |

influence so no diminishing of the matrix [*A*] was done unlike [1]. By replacing [*A*] by [*A*]/2, the differences on the computed residual strength are given Table 3. The differences are less than 10% and mostly situated between 0% and 5%, showing that the influence of membrane stiffness hypothesis is weak. The same discussion arises with the hypothesis on the bending stiffness matrix. Thus, computations were made with no delamination, 1 delamination (reference case Table 2) and three delaminations (Matrix [*B*] and [*D*] divided by 16). The results of the simulations are shown Fig. 10. With no delamination, by comparison with one delamination, the residual strength given by the criterion is increased from 3% to 20% and with three delaminations the residual strength is decreased from 0.4% to 15%. The sensitivity is generally less than ±5% on thin skins (0.4 mm and 0.8 mm) and is more important for the 1.2 mm thick one (cases 7 and 8). This hypothesis seems weak for the skins less than 0.8 mm thick but will be more and more sensitive for thicker skins. However, for the cases analysed, the proposed reduction in stiffness seems to be the better approximation. Generally speaking, it seems that the stiffness reduction of the skin is not the main factor for thin skins. The compression after impact phenomenon seems due to the geometric nonlinear behavior caused by the shift of the neutral plane due to the dent and to the nonlinear response of the core.

A very important hypothesis made was the estimation of the crushed core depth $\delta_C$. In the case studied, the values were obtained by destructive sectioning [1,17]. It will no longer be possible for impacts occurring on flying parts. Thus, from the values given, a variation of ±50% was tested and the influence on the residual

**Table 3**
Influence of the membrane stiffness of the damaged skin

| Test | Test 1 | Test 2 | Test 3 | Test 4 | Test 5 | Test 6 | Test 7 | Test 8 |
|---|---|---|---|---|---|---|---|---|
| [*A*]/2 | −7% | −10% | +3.4% | 0% | 0% | +5% | 0% | +5% |

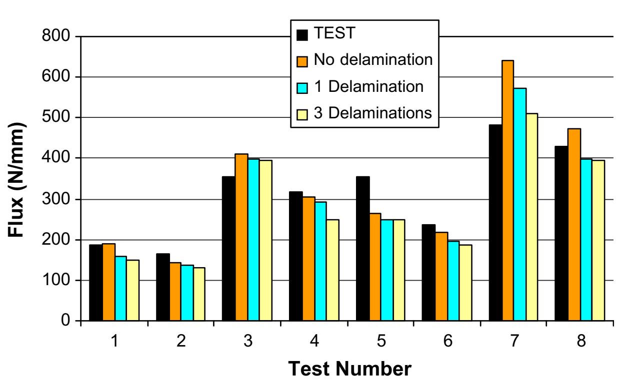


**Fig. 10.** Bending stiffness in the damaged skin influence.

**Table 4**
Influence of crushed core depth

| Test | Test 1 | Test 2 | Test 3 | Test 4 | Test 5 | Test 6 | Test 7 | Test 8 |
|---|---|---|---|---|---|---|---|---|
| $\delta_C$ + 50% | +1% | −4.5% | 0% | 0% | −2.6 % | 0% | −3.5% | 0% |
| $\delta_C$ − 50% | 0% | 0% | +3.4% | 0% | + 2.6% | +24% | +3.5% | +5% |

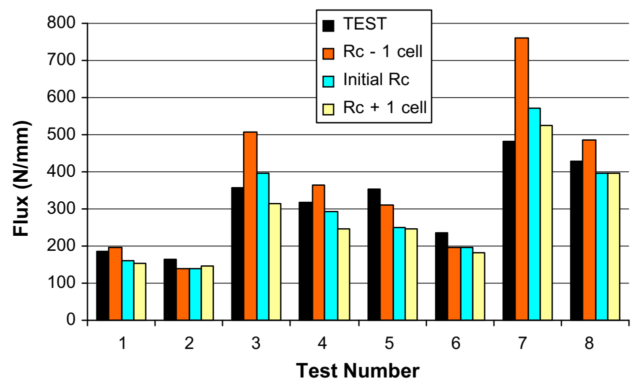


**Fig. 11.** Core crush radius influence.

strength computed is shown Table 4. Clearly, the variation is less than 5% except in one case (no. 6, −50%) with a rise of 24%. However, in this case the impact-damaged area is wide and deep. Therefore, a reduction in the crushed core depth increases the stiffness of the core and the skin cannot compress it in the same manner, thus rising the critical load. To confirm this explanation, an additional test was computed by arbitrarily setting the core crushed depth to 0.1 mm in cases 4 and 8, and the increase in the critical load was up to 50%. Thus, it is simply necessary enough to estimate the core depth to obtain accurate results. In practise, this can be done by using the data already available in any aircraft company. A doubt also exist on the measurement by NDI of the core crushed radius $R_C$ and the value finally used especially for minor damage. Thus, a sensitivity study on this radius was carried out by varying the radius value of +/1 cell diameter (4.76 mm). The computation results are given Fig. 11. Diminishing this radius increases significantly the strength, except for case nos. 2 and 6. That is normal, since, for those two cases, the damage is already large. Increasing this radius has a little influence, except in cases 3, 4 and 7 where the damage area is rather small. In case no. 3, the influence is sufficient to correlate the test. Generally, the crushed core radius has an important influence on the strength given by the criterion and thus, the given value has to be as close as possible to reality.

Overall, the strength given by the criterion is robust with respect to our hypotheses for the skin and the core. The main sensitiveness was found for the crushed core radius and it has to be measured carefully. Moreover, by changing different parameters, the strength predicted evolves following the expected mechanical behavior that confirms the pertinence of the criterion.

## 6. Conclusions

A new criterion to compute the compression after impact strength of sandwich structures with thin composite skins and Nomex honeycomb core is proposed. It is based on the crush of the first intact cell of the honeycomb located on the major axis of the ellipse caused by the residual dent progression under compression. A nonlinear finite element model using Mindlin plate elements for the skins and a grid of vertical nonlinear springs for the core was developed. It allows quick and accurate prediction of the residual strength of impact data available in the literature except in the cases of small impact dents. The main parameters of the model can be measured directly or by NDI techniques on real structures. For the other parameters, several assumptions were made and it was demonstrated that the criterion is robust. In particular, a relative insensitiveness to the crushed core depth was found since the initial value chosen was sufficient. This model involves a linear elastic response of the skins that is a strong hypothesis especially for thick skins. The model can be improved, in the case of progressive dent evolution, by combining it with a crack initiation criterion or by a delamination growth criterion as proposed by Lacy and Hwang [17]. Finally, the use of a grid of spring does not allow the modelling of the bending of sandwich structures and an improved model must be developed to take into account the loading of real structures.

## References


[1] Lacy TE, Hwang Y. Numerical modelling of impact-damaged sandwich composites subjected to compression after impact loading. Compos Struct 2003;61:115–28.

[2] Hooper EH. Starship: A model for future design. Materiaux et Techniques 1989;6:23–30.

[3] Sheahen P, Bersuch L, Holcombe T, Baron B. Robust composite sandwich structures. AIAA Paper Number A98-25225/ AIAA 98-1873.

[4] Abrate S. Localized impact on sandwich structure with laminated facings. Appl Mech Rev 1997;50(2):69–82.

[5] Tomblin J, Lacy T, Smith B, Hooper S, Vizzini A, Lee S. Review of damage tolerance for composite sandwich airframe structures. Federal Aviation Administration Report Number DOT/FAA/AR- 99/49.

[6] Castanié B, Barrau JJ, Jaouen JP, Rivallant S. Combined shear/compression structural testing of asymmetric sandwich structures. Exp Mech 2004;44(5):461–72.

[7] Tsang PW, Lagace PA. Failure mechanism of impact-damaged sandwich panels under uniaxial compression. Proc 35th AIAA/ASME/ASCE/AHS/ASC Struct Des Mater Conf 1994;2:745–54.

[8] Bernard ML, Lagace PA. Impact resistance of composite sandwich plates. J Reinforced Plast Compos 1989;8(9):432–45.

[9] Cvitkovich MK, Jackson WC. Compressive failure mechanism in composite sandwich structures. J Am Helicopter Soc 1999;44(4):260–8.

[10] Lagace PA, Mamorini L. Factors in the compressive strength of composite sandwich panels with thin facesheets. J Sandwich Struct Mater 2000;2:315–30.

[11] Tomblin J, Raju KS, Acosta JF, Smith BL, Romine NA. Impact damage characterization and damage tolerance of composite sandwich airframe structures – Phase II. Federal Aviation Administration Report Number DOT/FAA/AR-02/80.

[12] Minguet PJ. A model for predicting behavior of impact-damaged minimum gage sandwich panels under compression. AIAA Paper 1991 Number AIAA-91-1075-CP.

[13] Xie Z, Vizzini AJ. A feasible methodology for engineering applications in damage tolerance of composite sandwich structures. J Compos Mater 2004;38:891–914.

[14] Xie Z, Vizzini AJ. Impact damage propagation in a composite sandwich panel subjected to increasing uniaxial compression after low velocity. J Sandwich Struct Mater 2005;7:269–88.

[15] Guedra-Degeorges D, Thevenet P, Maison S. Damage tolerance of sandwich structures. Proc EUROMECH 360 Colloquium. Kluwer Academic Publisher; 1997.

[16] Zenkert D, Shipsha A, Bull P, Hayman D. Damage tolerance assessment of composite sandwich panels with localised damage. Compos Sci Technol 2005;65(15-16):2597–611.

[17] Lacy TE, Hwang Y. Numerical estimates of the compressive strength of impact-damaged sandwich composites. J Compos Mater 2007;41(3):367–87.

[18] Thomson RS, Mouritz AP. Skin wrinkling of impact-damaged sandwich composite. J Sandwich Struct Mater 1999;1:299–322.

[19] Aminanda Y. Contribution à l'analyse et à la modélisation de structures sandwichs impactées (2004). Ph.D. Dissertation of the Ecole Nationale Superieure de l'Aéronautique et de l'Espace (in French). http://theses.supaero.fr/001326.pdf.

[20] Aminanda Y, Castanié B, Barrau JJ, Thevenet P. Experimental analysis and modelling of the crushing of honeycomb cores. Appl Compos Mater 2005;12(3-4):213–27.

[21] Castanié B, Bouvet C, Aminanda Y, Barrau JJ, Thevenet P. Modelling of low energy/low velocity impact on nomex honeycomb sandwich structures with metallic skins. Int J Impact Eng 2008;35(7):620–34.

[22] Aminanda Y, Castanié B, Barrau JJ, Thevenet P. Experimental and numerical analysis of the compression after impact of metal-skinned sandwich structures. Compos Sci Technol 2007. doi:10.1016/j.compscitech.2007.10.045.

[23] Tomblin J, Raju KS, Acosta JF, Liew J, Smith JL. Impact damage characterization and damage tolerance of composite sandwich airframe structures. Federal Aviation Administration Report Number DOT/FAA/AR-00/44.

[24] Samcef User's Guide, by Samtech Group, Liege, Belgium. www.Samtech.com.